Appl. Phys. A 75, 559–563 (2002) / Digital Object Identifier (DOI) 10.1007/s003390101020

Applied Physics A
Materials
Science & Processing

The gas-sensing potential of nanocrystalline SnO_2 produced by a mechanochemical milling via centrifugal action

Ü. Kersen*

Laboratory of Electromechanics, Helsinki University of Technology, Otakaari 5A, P.O. Box 3000, Hut, Finland

Received: 25 July 2001/Accepted: 4 September 2001/Published online: 20 December 2001 – © Springer-Verlag 2001

Abstract. In this work, the synthesis of undoped nanocrystalline tin dioxide powders and the subsequent preparation of SnO_2 thick-films were studied. An initial mixture of $SnCl_2$ and $Ca(OH)_2$ was sealed in a vial for milling in an air atmosphere. Heat treatment of the milled powder resulted in the formation of tetragonal and orthorhombic SnO_2 phases, which was confirmed by X-ray diffraction (XRD) analysis. It was found that crystallite size could be controlled by varying the milling time, the rotation speed and the temperature used for the heat treatment. Crystallite sizes in the range 20 to 30 nm (determined by XRD measurements) were obtained. The total pore volume was 0.22 ml/g for a measured particle size of 37 m^2/g. No contamination of the powder during milling was found. The response of the prepared thick-films to H_2S gas in the concentration range 0.5 to 10 ppm in air was investigated as a function of the preparation conditions. The advantage of mechanochemical synthesis of powder is its relative simplicity, low cost and possibility of obtaining isolated, unagglomerated nanosized grains. It is shown that chemical reactions, which usually occur in the vibratory mill to produce the SnO phase, can also be initiated during a short processing time in the centrifugal mill.

PACS: 81.20.E; 81.20.W; 61.10.N; 07.07.D

It is known that one of the most important factors affecting the gas-sensitive properties of SnO_2 samples is the grain or crystallite size. This size is usually much larger than the depth of the space charge layer, and electrical conduction is controlled by the grain boundaries. Nanocrystalline powders, which may have a grain size less than 100 nm, are prepared at present using several methods such as sol-gel chemistry, thermal decomposition, physical vapor deposition, crystallisation of an amorphous precursor and gas condensation. An important problem with these methods is the control of the size of agglomerations.

*Corresponding author.
(Fax: +358-9-451-2991, E-mail: FjsnYlKr@netscape.net)

The synthesis of ceramic powders by mechanical milling and subsequent heat treatment comprises the content of mechanochemical processing (MCP) [1]. The repeated ball-powder collisions induce structural changes and continually regenerate the reacting interfaces. A chemical reaction can take place either during the milling process or in the furnace during the heat treatment stage. One advantage of the MCP method is that the synthesized powder has a large surface area and relatively good porosity, which is important for the application of this material in gas sensors. Also, the mechanochemically processed powder is not agglomerated by shape. This is because the formation of a by-product, often salt, encapsulates the separated tin dioxide nanoparticles, stopping their subsequent growth. Removal of the salt matrix is carried out using an appropriate solvent and a powder is obtained after drying. There are three common types of high-energy mills used in the MCP: planetary, attrition and vibratory. Most of the reports that have appeared in the literature have described the use of either vibratory or planetary mills. Mechanical alloying, a dry and high-energy milling process, involves repeated deformation, fracture, and welding of powdered particles and is a suitable tool for synthesizing materials on a large scale [2].

In contrast to the high-energy alloying described above, the present study shows that it may be possible to obtain powders of nanosized particles using a centrifugal mill of the conventional type. The effect of milling conditions on powder quality were investigated, including the milling time and rate, the mass ratio of the balls and powder and the amount of salt required to be added to the starting material before processing.

The important factor, associated with the sensing properties of a prepared SnO_2 thick-film, is the grain size and geometry of connection [3]. For grain sizes much less than 20 nm, the sensitivity to a reducing gas is significantly increased [4], as the grains will be depleted of electrons and the gas response is related to intergrain conduction. Further improvement in the response may be obtained if the depletion layer thickness is close to the radius of the grain, typically measured to be about 6 nm [5]. The responses of sensorsmade from films of SnO_2 grains prepared using MCP are reported.

1 Experimental

Nanosized SnO_2 powder particles were produced by mechanochemical synthesis, where the milling process was performed at room temperature in a centrifugal-type mill. To date, most authors have used vibratory mills (Spex 8000) or planetary type mills (Fritsch P5 or P7) for this process. The chemical reaction induced was

$$SnCl_2 + Ca(OH)_2 \rightarrow SnO + CaCl_2 + H_2O\,. \quad (1)$$

The starting materials (4.7 g of $SnCl_2$, 1.83 g of $Ca(OH)_2$ and 8.92 g of $CaCl_2$) were sealed in a non-metallic vial in an air atmosphere and milled to produce 10 g of SnO. Milling was performed using steel balls with a diameter of 12.7 mm. Two ball-to-powder mass ratios were used, the first of 3:1 with a rotation speed of 75 rpm and the second of 5:1, with a speed of 100 rpm. The milled powder was subsequently heat treated at 400 °C for 1 h in an air atmosphere to complete the SnO_2 formation. Removal of the $CaCl_2$ by-product was carried out with deionised water using an ultrasonic bath and a centrifuge. The washed powder was dried in a furnace at 65 °C for 8 h.

A Philips PW 1830 X-ray powder diffractometer with Cu K_α radiation was used to follow the crystallisation of the powder as a function of heat treatment temperature. X-ray analysis was important for the confirmation of the microstructure of the synthesized powder obtained after washing and removal of all $CaCl_2$ (both added and produced in the reaction). The SnO_2 crystallite size was determined using Scherrer's equation [6]. The specific surface area and porosity of the synthesized powders were measured with a Coulter Omnisorp 100CX, using a N_2 gas adsorption method at 77 K. The surface area was obtained by assuming particles to be spherical.

Thick-film gas sensors were prepared by conventional hand coating of a paste, the SnO_2 powder mixed with an α-terpineol-based solvent, over the Au sensing electrodes on an Al_2O_3 substrate. Subsequently, these substrates were sintered at 500 °C, 600 °C and 700 °C for 1 h in air and one thick film was sintered at 700 °C for 1 h in a N_2 gas flow. Pt wires were attached to the pads of the heater and sensing electrodes by using an Au paste and heat treatment. The gas response tests were carried out with a PC-controlled measuring system. Sensors to be tested were placed in a measuring chamber of about 0.5 l in volume. Optimum detection temperatures were determined and thick-film sensors maintained at these fixed temperatures were exposed to varying test gas concentrations of H_2S in the range 0.5 to 25 ppm, using a gas flow controller unit with an air flow rate of 0.5 l min^{-1}. Sensitivity, S, to gas is defined as,

$$S = \left(R_{air} - R_{gas}\right) / \left(R_{air}\right) \cdot 100\%\,, \quad (2)$$

where R_{air} is the sensor resistance in clean air and R_{gas} is the resistance in the test gas.

2 Results and discussion

For the first milling condition examined, the milling time was kept at four hours, the relationship of ball-to-powder mass was 3:1 and the rotation speed was maintained at 75 rpm. The mixture obtained from this was heat treated at 400 °C for 1 h resulting in the exothermic reaction:

$$SnO + 1/2(O)_2(g) \rightarrow SnO_2\,. \quad (3)$$

An XRD pattern of the synthesized powder, after removal of the $CaCl_2$ mass and drying, is presented in Fig. 1. The tetragonal phase is clearly dominant, with the orthorhombic phase giving rise to only two very weak peaks. It may be concluded that the crystallisation has succeeded at this low temperature of 400 °C. The three main peaks are located at 26.6, 33.9, and 51.8 degrees respectively and show a high degree of crystallinity. The crystallite size, D, was calculated according to the Scherrer equation,

$$\Delta\,(2\theta) = K\alpha / \left(D\cos\theta\right) \quad (4)$$

where $\Delta\,(2\theta)$ is the width at half-maximum intensity (in radians) and θ is the Bragg angle of the (110) plane in the diffraction pattern of the peak, K is a constant, depending on the line shape profile (currently $K = 1$), α is the wavelength of the X-ray source (in the case of Cu radiation, $\alpha = 1.54059$ Å) and D is the crystallite size. The most intense peak, the (110) tetragonal peak, was chosen to minimise the error introduced from the overlap of peaks from the tetragonal and orthorhombic phases.

An increase in milling time results in the decrease in powder crystallite sizes, as seen in Fig. 2. Nevertheless, the XRD crystallite size evolution on increasing the milling time from 2 to 6 h seems to be limited, and it is necessary to change the milling conditions, because it is likely that a milling time of more than 6 h will not reduce the crystallite size greatly. Some degree in reduction of crystallite size can be obtained by heat treating below 400 °C, as shown in Fig. 3. Above this temperature, the crystallite size moderately increases in the temperature range 300 °C to 500 °C, but heating at higher temperature causes much faster crystallite growth.

An interesting relationship between the synthesized crystallite size and the amount of $CaCl_2$ added to the reagents before the milling is presented in Fig. 4. Here the milling conditions have been modified: the ball-to-powder mass ratio was 5:1, and a rotation speed of 100 rpm was used. For minimum

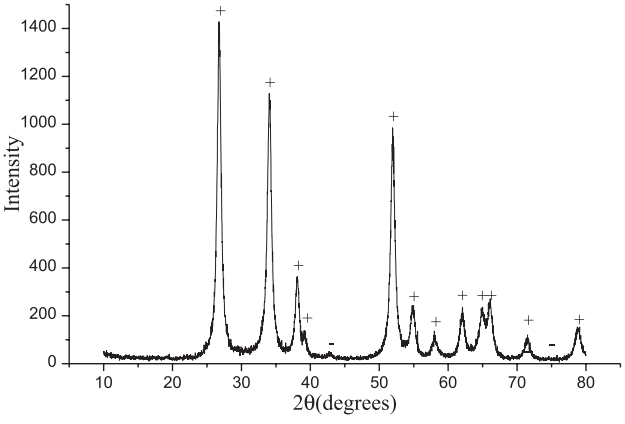

Fig. 1. X-ray diffraction pattern of the synthesized SnO_2 powder (8.92 g of $CaCl_2$ in the milling composition) with the typical distribution of tetragonal (+) and orthorhombic (−) phases

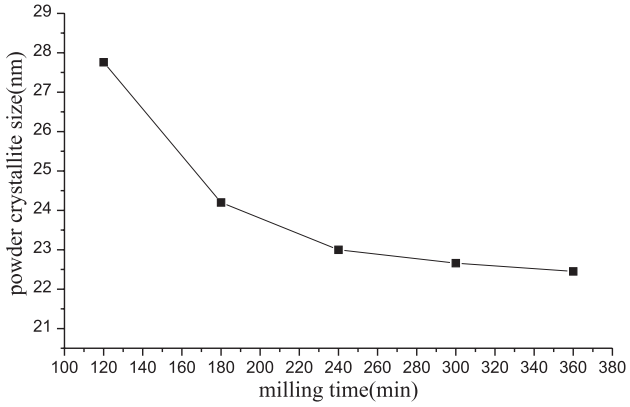

Fig. 2. Synthesized crystallite size evolution as a function of the milling time. After processing in a ball mill, all milling compositions were heat treated at 400 °C for 1 h and salt the matrix was removed

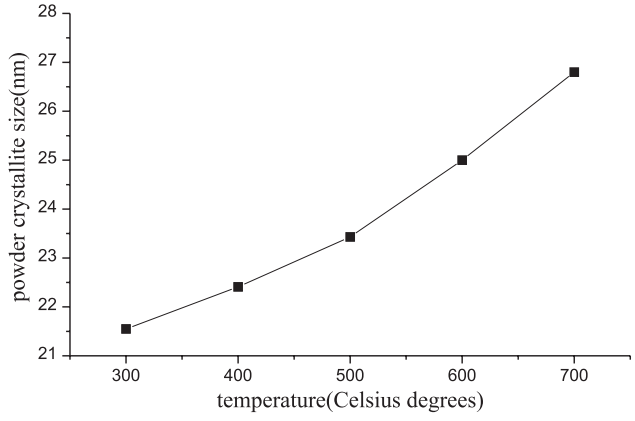

Fig. 3. Synthesized crystallite size evolution with higher heat treatment temperature. All milling compositions were milled for 4 h

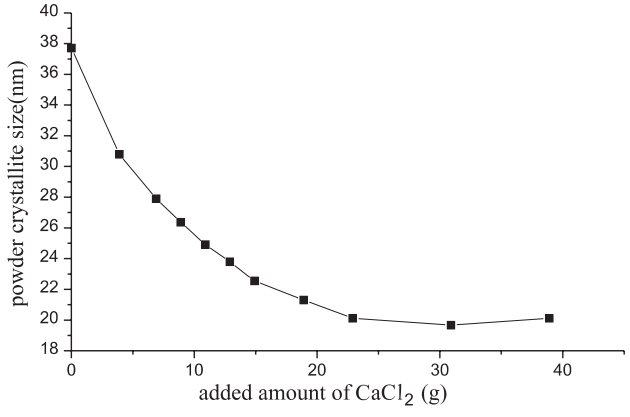

Fig. 4. Synthesized crystallite size evolution as a function of $CaCl_2$ mass in milling composition. The relationship of ball-to-powder mass was maintained at 5:1 and the rotation speed at 100 rpm

particle sizes, about 20 nm, 30.9 g of salt is needed. However, it should be noted that the addition of large amounts of salt requires a much longer washing procedure. The powder X-ray diffraction patterns for two different masses of salt removed are presented in Figs. 5, 6. There is no noticeable shift in the angle for the corresponding tetragonal and orthorhombic peaks in these figures, but the surface crystallisation process performed at 400 °C has resulted in different degrees of crystallinity. It is clearly seen from this work that prolonged milling causes crystallites and particle size to decrease considerably if there is a sufficient amount of salt surrounding the particles during the milling. Also, it seems that the porosity of the powder is increased by having a much longer processing time, while the crystallinity of the surface is decreased. Thus, by selecting the appropriate milling conditions, it is possible to obtain a more acceptable surface structure for subsequent gas sensor applications.

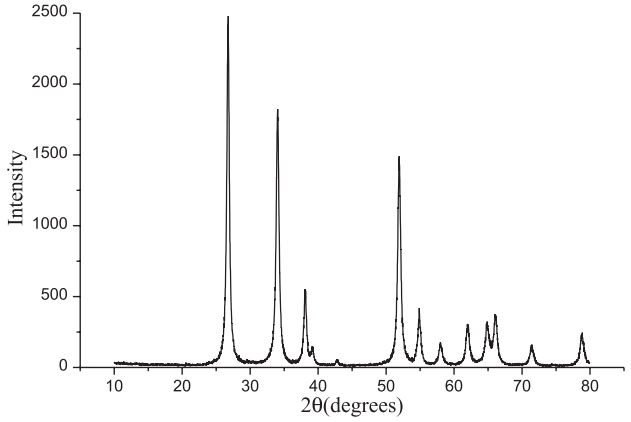

Fig. 5. X-ray diffraction pattern of the synthesized SnO_2 powder (3.9 g of $CaCl_2$ in the milling composition)

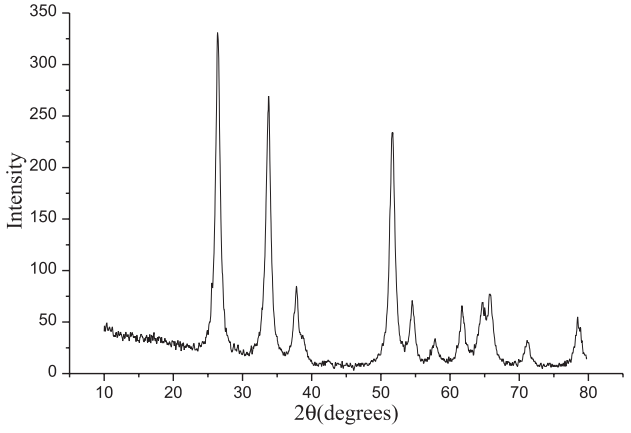

Fig. 6. X-ray diffraction pattern of the synthesized SnO_2 powder (30.9 g of $CaCl_2$ in the milling composition)

As mentioned before, the series of pure thick films were prepared and sintered in air and in nitrogen within the range 500–700 °C. These thick films revealed a moderately good response and recovery times dependent on operating temperature. Fig. 7 represents a typical response of a SnO_2 thick-film sensor, operating at temperature of 250 °C and exposed to 10 ppm of gas. Both response and recovery times can be determined to be 15 min. The maximum sensitivity to H_2S may be viewed as a function of the sintering conditions as shown in Figs. 8, 9 below. The sensitivity to H_2S is to a large degree influenced by changes in the sintering temperature. Firing at higher temperature gives rise to a sensing film. Comparing with previous work on tin oxide ceramics [7], sintering in the temperature range 500 to 700 °C does not substantially change the average pore size, but above this temperature range the pore size begins to grow. Although the grain size

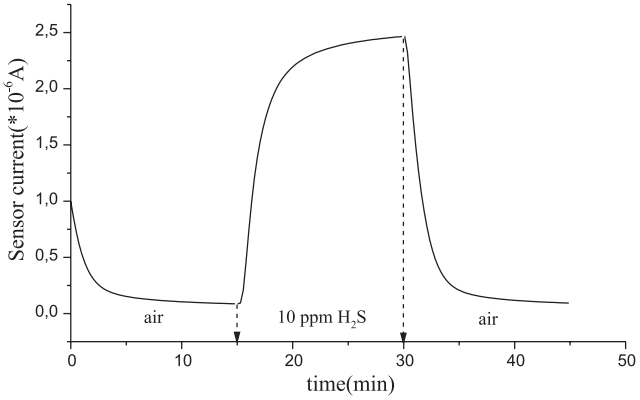

Fig. 7. Response of the thick film sintered at 700 °C for 1 h to 10 ppm of H_2S gas in air

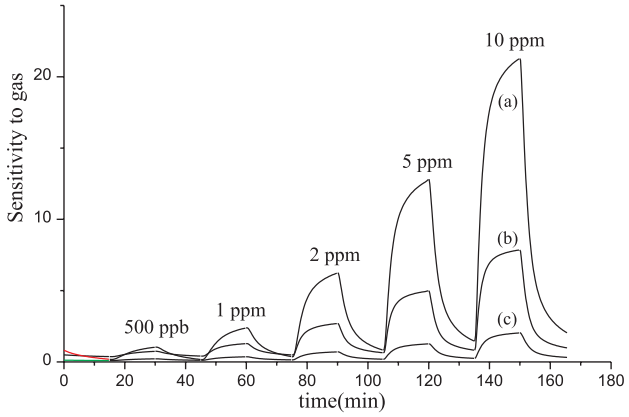

Fig. 8. Dynamic response of SnO_2 thick films sintered at 500 °C (a); 600 °C (b); and 700 °C (c) in an air atmosphere for 0.5 h to increasing concentrations of H_2S gas in air

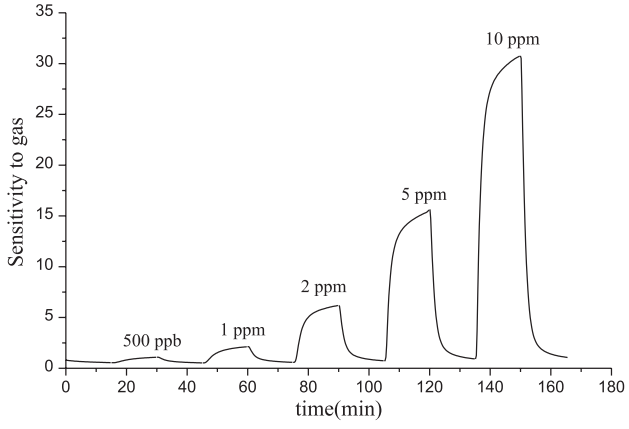

Fig. 9. Dynamic response of a SnO_2 thick film sintered at 700 °C in an N_2 atmosphere for 0.5 h to increasing H_2S concentrations in air. An air flow rate was kept at 0.5 $l min^{-1}$

of the thick film increases at higher sintering temperature, the observed enhanced sensitivity to gas ($S = 20$, curve (a) in Fig. 8) can be explained by the greater porosity produced by sintering at 700 °C.

It is known that a change in oxygen partial pressure causes a change in oxygen vacancy concentration in these samples. Sintering in a reducing gas atmosphere at lower temperature may remove bridging oxygen, while use of higher temperature removes oxygen on the surface. H_2 is occasionally used as an effective reducing gas [8], but due to its explosive character it is not widely used and a better alternative could be to use N_2 gas. Sintering at 700 °C for 1 h with this and using a flow rate of 50 ml min^{-1} yields non-stoichiometric SnO_{2-x}, where x denotes the oxygen deficiency. The nitrogen cylinder used for sintering this thick film layer has, in addition to nitrogen gas, a very low oxygen content of about 0.1 ppm O_2, which is equivalent to a considerably reduced $p(O_2)$. Heating to temperatures above 500 °C starts a substitution of removed bridging oxygen with oxygen vacancies ($V_o^{\cdot\cdot}$) [9]. In SnO_{2-x}, these defects are majority carriers and are charge compensated by conduction electrons (e'). The oxygen exchange equilibrium may be written as

$$O_o = V_o^{\cdot\cdot} + 2e' + 1/2O_2(g) \quad (5)$$

where O_o represents lattice oxygen. Since the formation of Schottky defects may occur at higher temperatures, these are not used [10].

One can see in Fig. 9 that good gas-sensitivity was achieved, with sensitivity $S = 33$ upon exposure to 10 ppm of H_2S. This is due to the increased concentration of oxygen vacancies on the surface, caused by sintering in the nitrogen atmosphere instead of air. It can be seen in Fig. 7 that the response time to 10 ppm of gas is 5 min (at the level of 0.9). There are few results in the literature on the response time of SnO_2 materials to H_2S gas. Some authors [11] have not presented their measured quick dynamic responses (below 1 min) and/or that response has not been sufficiently fast (over 1 h) [12]. Although the total measured pore volume of the synthesized powder was 0.21 ml g^{-1}, it seems that sintering at a higher temperature has nevertheless resulted in loss of porosity to some degree, resulting in the sintered microstructure not having sufficient porosity and causing the response time to be prolonged by up to 5 min. It is obvious that replacing the grinding phase by ball milling of the synthesized powder results in less agglomeration and a film with a more porous structure.

3 Conclusions

Mechanochemical processing in a centrifugal action of predetermined stoichiometric amounts $SnCl_2$ and $Ca(OH)_2$ in an excess of $CaCl_2$ resulted in the formation of the desired mass of SnO. After separation, non-agglomerated particles were oxidised to SnO_2 powder with a tetragonal phase. The quality of the synthesized powder was determined by the energy input: the ball-to-mass weight relationship and the milling time. It was shown that SnO_2 processing is possible in air, i.e. without the requirement of an argon or a nitrogen atmosphere and this resulted in no contamination of the powder from the vial. The SnO_2 thick-film sensor's response to H_2S gas may be improved by: 1) synthesising powder grains smaller than 15 nm by using more input energy for the milling; 2) introduction of a grinding phase for the synthesized powder before paste preparation; and 3) using a screen-printing technique instead of hand-coating to produce thinner films. The long-term stability of the sensor and cross-sensitivity to O_2, H_2O, CO and other reducing gases remains a topic for future work.

Acknowledgements. The author is thankful to Dr. G. Darling, Surface Science Research Centre, University of Liverpool, for his help on preparing the manuscript.

References

1. T. Tsuzuki, P.G. McCormick: Physica B **239**, 378 (1997)
2. P.G. McCormick, F.H. Froes: JOM **50**, 61 (1998)
3. C. Xu, J. Tamaki, N. Miura, N. Yamazoe: Denki Kagaku **58**, 1143 (1990)
4. T. Nakahara, H. Koda: *Chemical Sensor Technology*, Vol. 3 (Kodansha and Elsevier, Amsterdam, 1992)
5. C. Xu, J. Tamaki, N. Miura, N. Yamazoe: Sens. Actuators B **3**, 147 (1991)
6. B.D. Cullity: *Elements of X-ray Diffraction*, 2nd edn. (Addison-Wesley, Reading, MA, 1978)
7. H. Torvela, T. Jaakola, A. Uusimäki, S. Leppävuori: J. Electron. Mater. (AIME) **15**, 1, 7 (1985)
8. D. Wang, J. Jin, D. Xia, Q. Ye, J. Long: Sens. Actuators B **66**, 260 (2000)
9. I. Manassidis, J. Goniakowski, L. Kantorovich, M.J. Gillan: Surf. Sci. **339**, 258 (1995)
10. B. Kamp, R. Merkle, J. Maier: Sens. Actuators B **3916**, 1 (2001)
11. G. Fang, Z. Liu, C. Liu, K. Yao: Sens. Actuators B **66**, 46 (2000)
12. M. Rumyantseva, M. Labeau, G. Delabouglise, L. Ryabova, I. Kutsenok, A. Gaskov: J. Mater. Chem. **7**, 1785 (1997)